

Three-dimensional magnetic reconnection simulations using the Eulerian Conservative High Order (ECHO) code.

Simone Landi

Dipartimento di Astronomia e Scienza dello Spazio, Università di Firenze

In collaborazione con:

Pasquale Londrillo

INAF-Osservatorio Astronomico di Bologna

Luca Del Zanna

Dipartimento di Astronomia e Scienza dello Spazio, Università di Firenze

Marco Velli

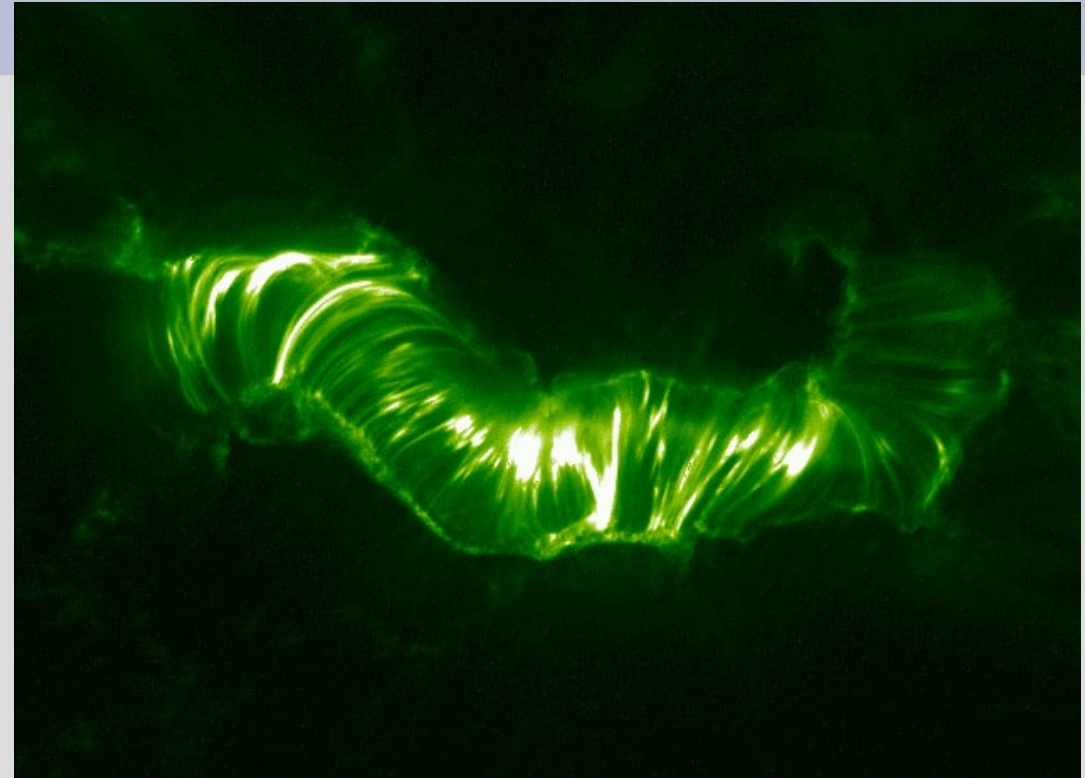
Dipartimento di Astronomia e Scienza dello Spazio, Università di Firenze

Introduction

Magnetic reconnection is a pervasive phenomenon in the outer solar atmosphere, solar wind and heliosphere.

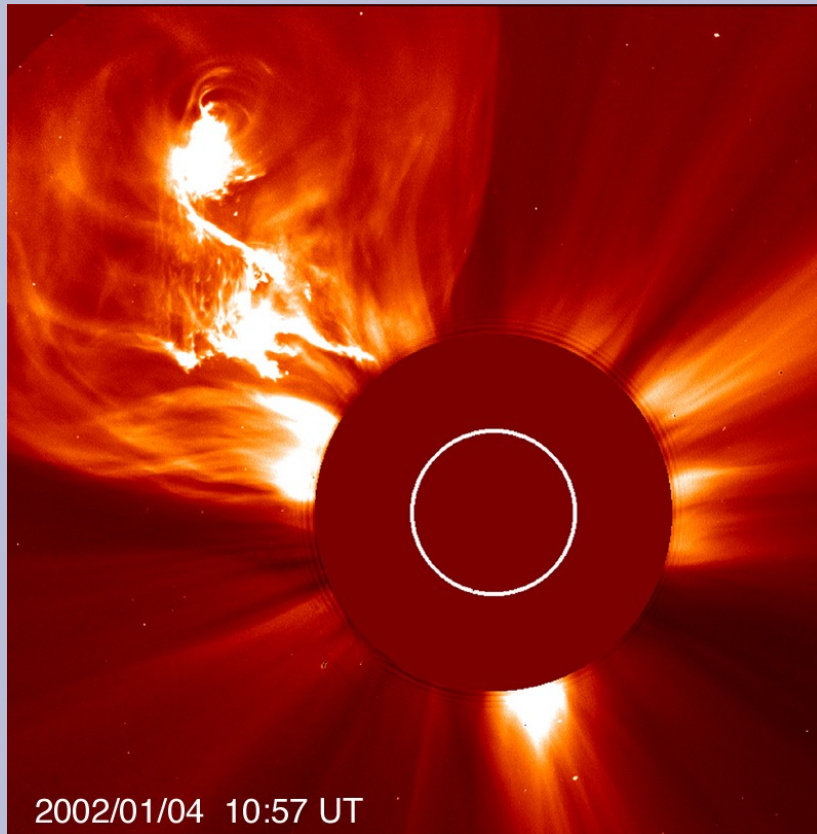
Fundamental in understanding several phenomena in the Heliosphere such as:

- Explosive phenomena (e.g. Solar Flare)
- Coronal heating
- Observed Structures in the Heliosphere
- Properties of turbulence and particle transport

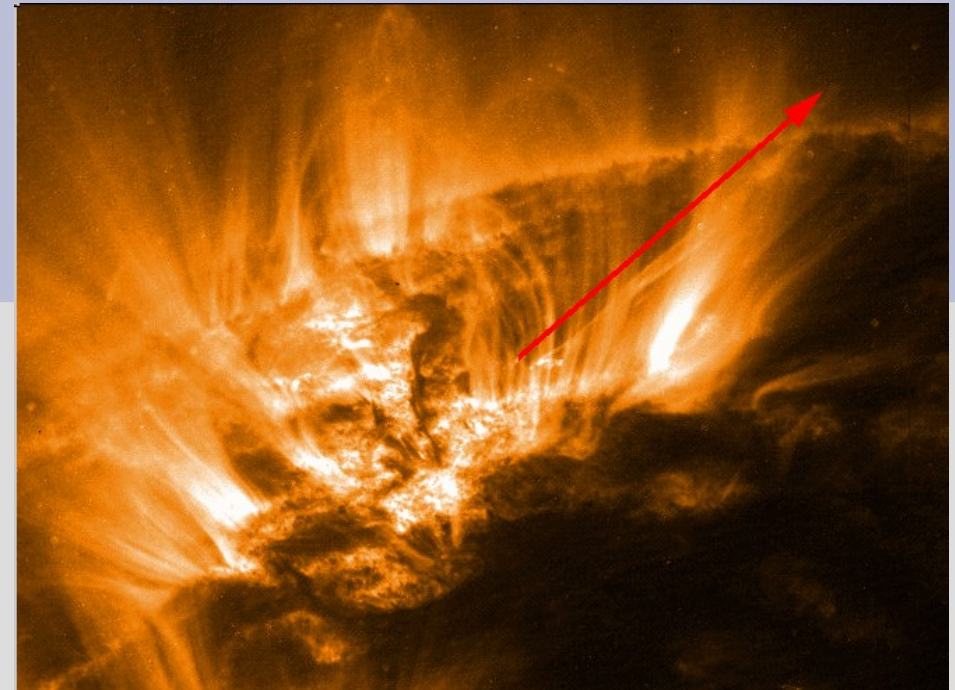


A solar flare occurred on July 14, 2000, observed by TRACE at the 195Å pass band . Field of view is about 250,000km by 170,000 km. Typical timescales are of order of 1-10 min. The energy released is up to 10^{33} erg

Fast inhomogeneous plasma flows are ubiquitous in the heliosphere, as result of acceleration in the solar corona and from reconnection itself.



A Coronal Mass Ejection (CME) as seen by LASCO-C2 coronagraph on board of SOHO. Typical velocities are of the order of 1000 km/s.



Small plasma ejections (indicated by the red arrow) inside an active region on the Sun and originating in a emerging magnetic field flux. Plasma blobs are ejected at about 600 km/s. Image taken by TRACE in the 171 Å passband.

The combined effect of resistive and KH-like instabilities may lead to much of the phenomenologies observed in the solar atmosphere

In treating heliospheric plasma we are faced with low and/or moderate values of the plasma beta => **reconnection flows are supersonic**

Usually the basic solar wind structure has differential shears that can exceed both sound and Alfvén speeds (5 to 10 times greater)

We need compressible and resistive MHD with:

- **Shock-capturing numerical schemes**, relevant for high Mach number flows and to follow the steepening of compressive modes and
- **High order numerical approximation**, to better resolve small scale turbulent activity and to resolve explicit dissipative terms.

Overview

The ECHO code:

- General characteristics
- Inclusion of resistivity
- Importance of using high-order schemes in non ideal MHD problems

Two applications:

- 3D simulations of compressible tearing instability
- 3D simulations of jet + current sheet instabilities

Conclusions

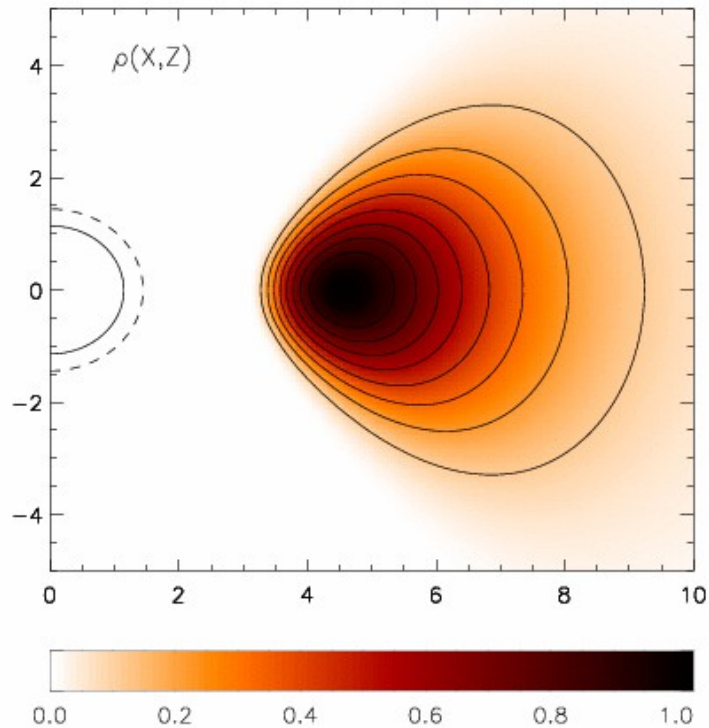
ECHO code

Eulerian Conservative High Order

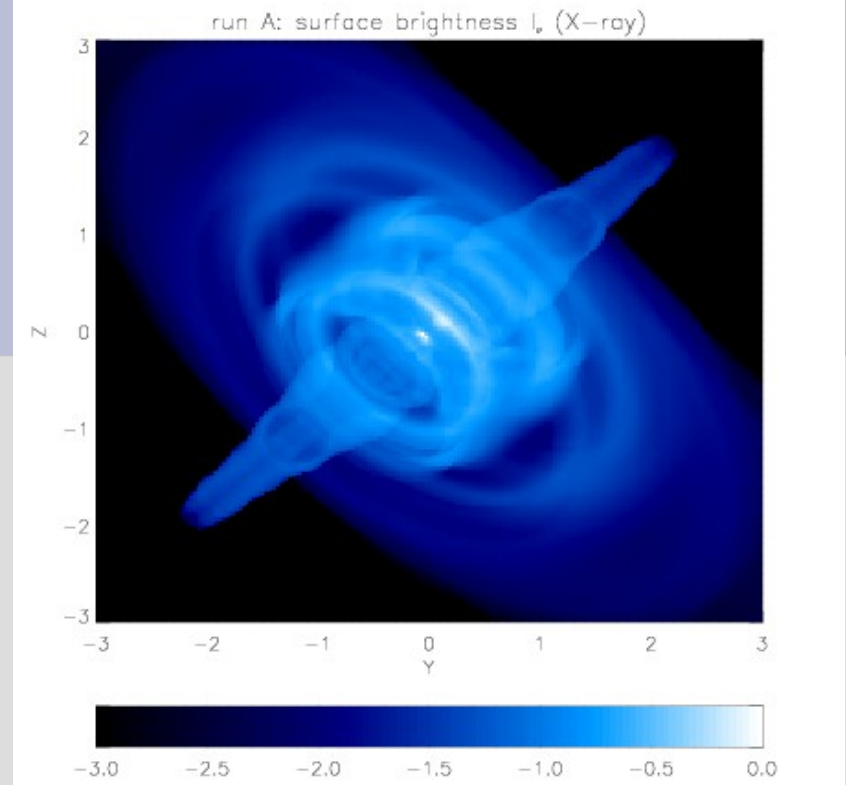
- Based on the **UCT** (Upwind Constrained Transport) method for threatening the solenoidal condition for the magnetic field (Londrillo & Del Zanna, 2000, 2004).
- High-order component wise **RE**Construction
- **HLL** (Harten, Lax & Van Leer, 1983) or Lax-Friedrichs (**LLF**) approximate Riemann solver
- High-order approximation of flux **DER**ivatives
- High-order **INT**erpolation procedures for staggered magnetic field
- 3rd or 4th order **Runge-Kutta** time stepping

ECHO solve different set of equation for magnetized fluids: **MHD**, **RMHD** and **GRMHD**

See poster Del Zanna et al.



Accretion disk around a black hole simulated with ECHO



Sintetic X-ray emission of a Pulsar Wind Nebula obtained by using the Relativistic MHD module of ECHO

To study magnetic reconnection processes and current-flows interactions we have included an **explicit resistivity** in the MHD System of equations

The electric field **E**

$$\mathbf{E} = -\mathbf{v} \times \mathbf{B} + \frac{c}{\sigma} \mathbf{J} = -\mathbf{v} \times \mathbf{B} + \eta \nabla \times \mathbf{B}$$

and the energy flux **H**

$$\mathbf{H} = \mathbf{v} \left(e + p + \frac{1}{2} B^2 \right) - (\mathbf{v} \cdot \mathbf{B}) \mathbf{B} - \frac{c}{\sigma} \mathbf{B} \times \mathbf{J}$$



Resistive terms

depend now on the current density **J** via the collisional conductivity σ

The components of **J** are approximated with a high-order central finite-difference scheme (no upwind). Consistent if:

- Resistivity sufficiently large to be appreciated respect to the numerical diffusivity $\sim 1/\Delta X^r$
- Sufficiently small to be effective at the smallest resolved scales.

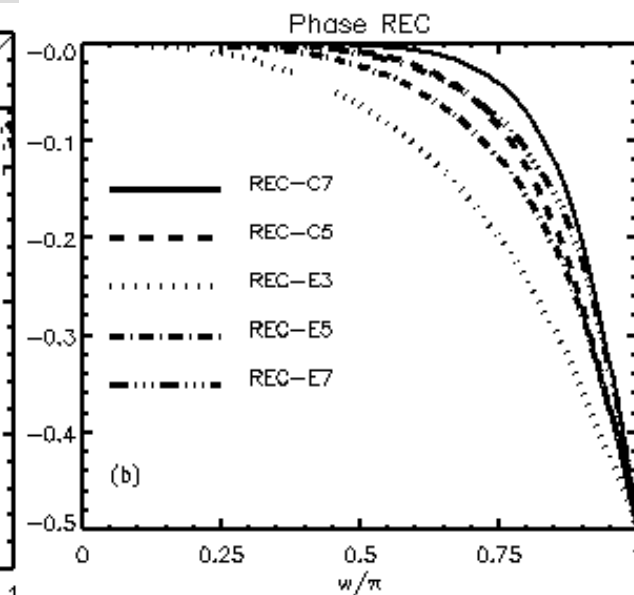
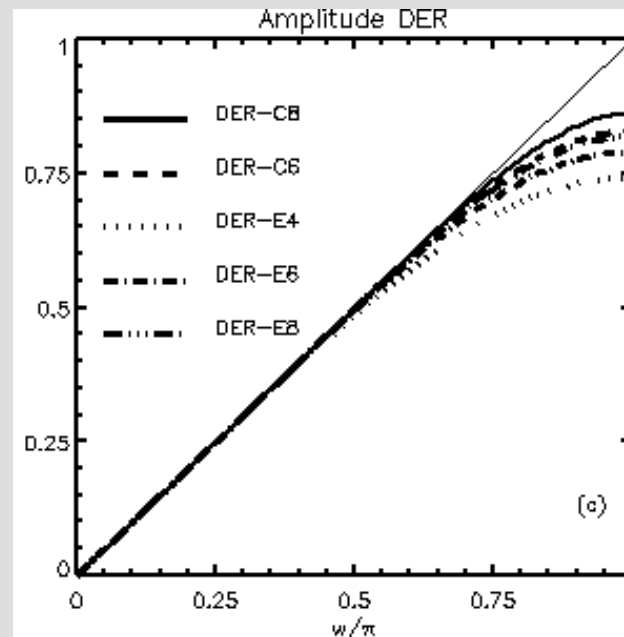
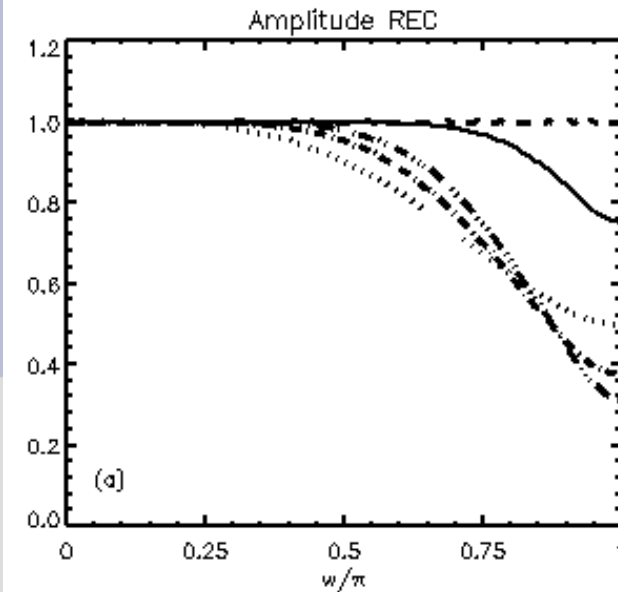
REC procedures:

- Explicit (E) and implicit (C) (Lele, 1992) procedures at various orders (3-7th) with a proper limiter (Suresh & Huynh, 1997).
- WENO (Liu et al., 1994) at various orders (3rd-7th).
- TVD & CENO3 (Liu & Osher, 1998)

DER and INT procedures:

- Explicit and implicit at various orders (4th-8th)

Spectral properties depend on the adopted procedures



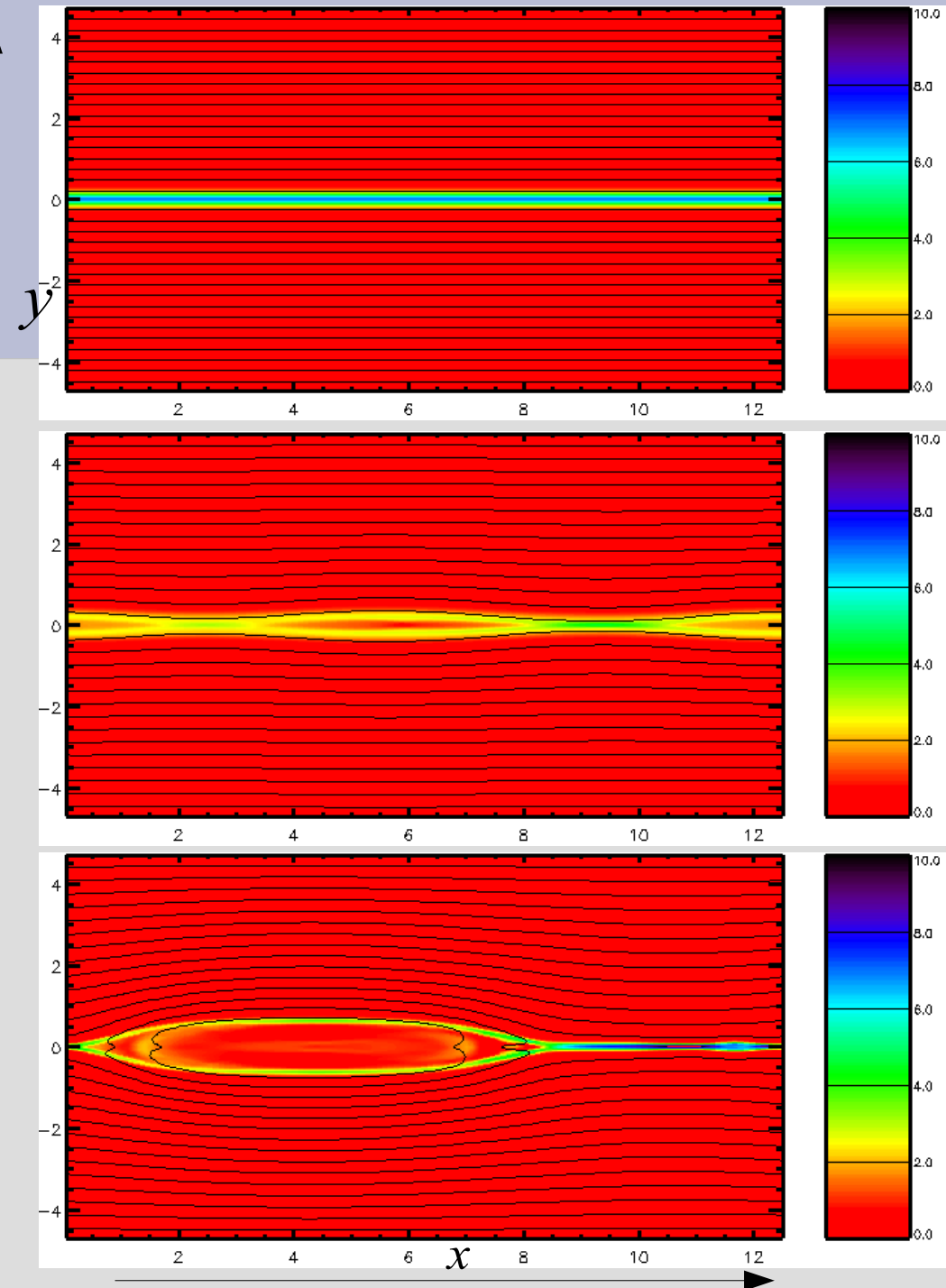
Right: Amplitude and phase of a reconstructed variables as function of the normalized wave-vector. An ideal reconstruction would be 1 for the amplitude and 0 for the phase. **Left:** Same plot for the DER procedure: here the exact derivation is the solid thin line.

A test: 2D tearing instability

In a current sheet, a well-known process associated with the magnetic diffusivity is the tearing instability (Furth et al., 1963).

The linear stage is characterized by the growth of resistive modes and formation of magnetic islands

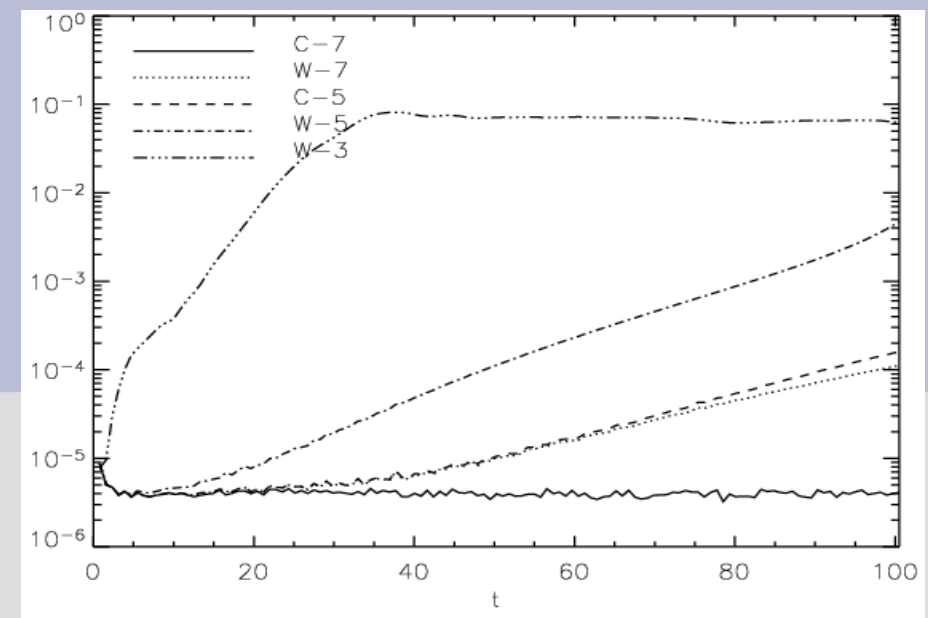
Magnetic islands are subjected to the coalescence process with formation of islands with larger and larger size (Hayashy, 1981; Malara et al., 1991)



Time evolution of the 2-D tearing instability:
magnetic field line and current density (color scale)

In simulating the tearing instability we have to take into account the numerical diffusivity introduced by the adopted numerical scheme.

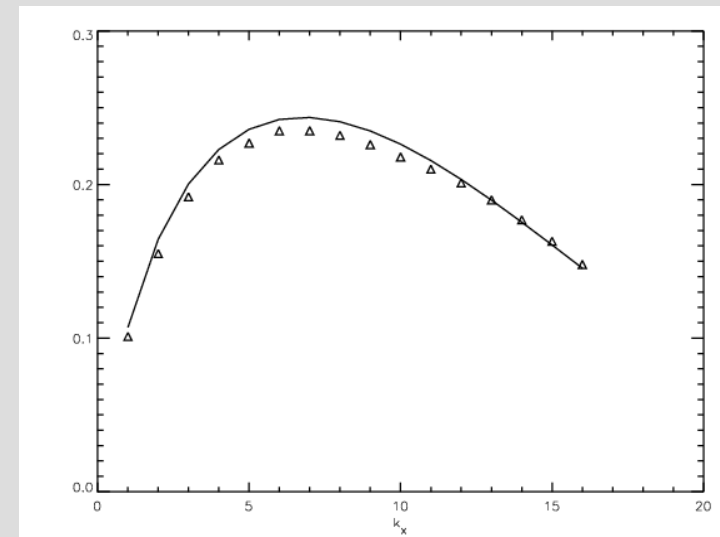
$$R_\eta = \infty$$



Test on the numerical dissipation for various schemes allowed by the code. It is measured the global fluctuating energy as function of time for a configuration where explicit magnetic diffusivity is zero.

Compact schemes (C-5, C-7) have either lower or null numerical dissipation. Higher dissipation is observed in using explicit WENO schemes (W-3, W-5, W7).

$$R_\eta = 5000$$



Comparison between the dispersion relation predicted by the linear theory (solid line) and those using the a 7th order compact scheme with ECHO.

We have verified that higher order scheme (especially compact schemes) are able to reproduce correctly the linear evolution of the tearing instability.

Application: 3D tearing instability

- Up to now: Incompressible MHD simulations (Dahlburg et al., 2002; Onofri et al., 2004)

Typical evolution in 3D:

- Linear tearing --> Inverse cascade (Coalescence) --> **Secondary Ideal 3D instability** (Dahlburg et al, 1992)

Our study (Landi et al., 2008)

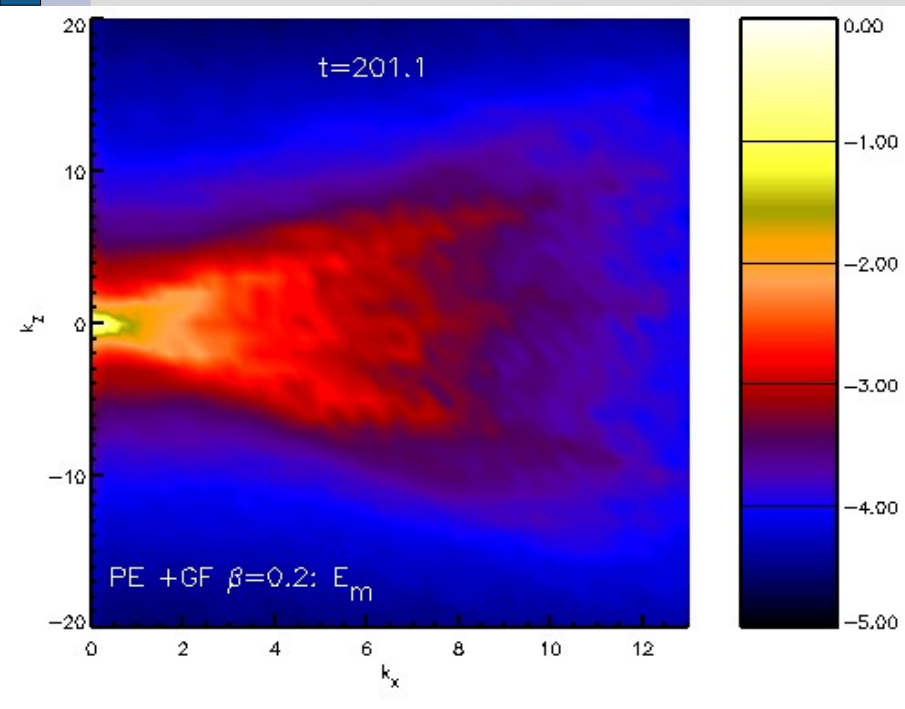
- Compressible MHD with different plasma beta regimes (high and low)
- Different initial configuration of the current sheet: Pressure equilibrium (PE) and Force-Free (FF) equilibrium

Non linear saturated state depends on the initial configuration

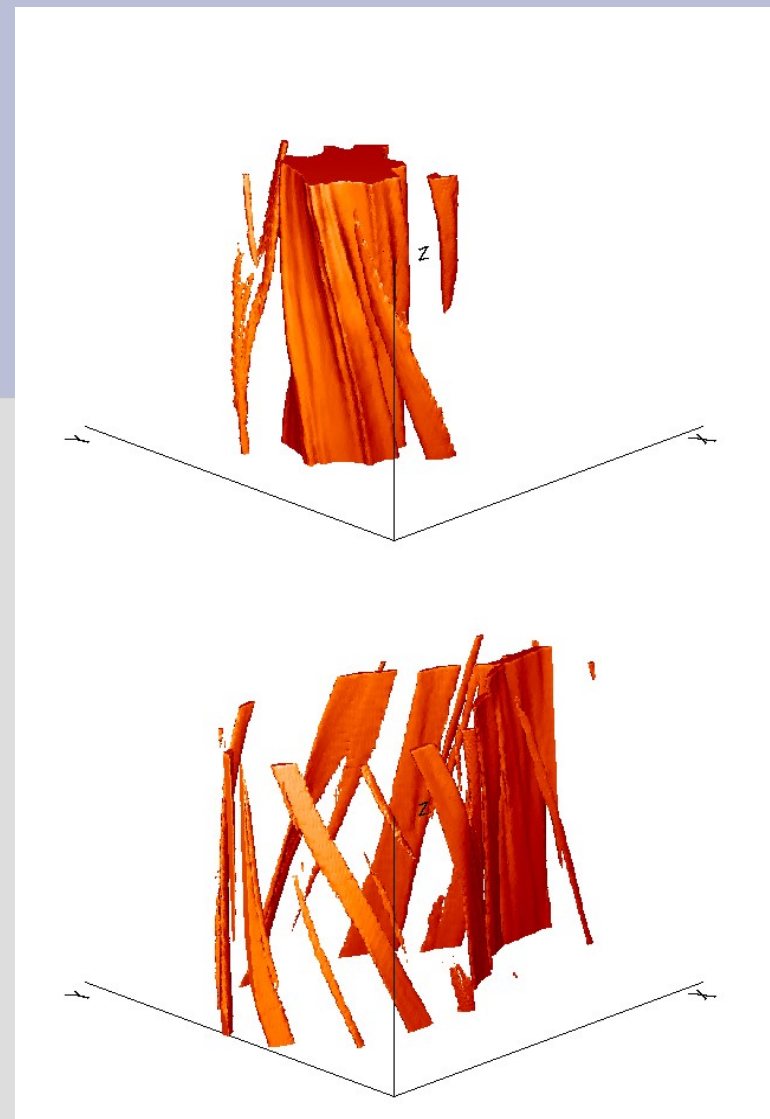
1-Pressure equilibrium configuration with guide field

Dynamics dominated by a typical coalescence process:

- Formation of magnetic islands with enhanced plasma pressure
- Presence of a current sheet which connects the two sides of the magnetic island.



Magnetic power spectrum in the (x-z) plane in the non-linear regime

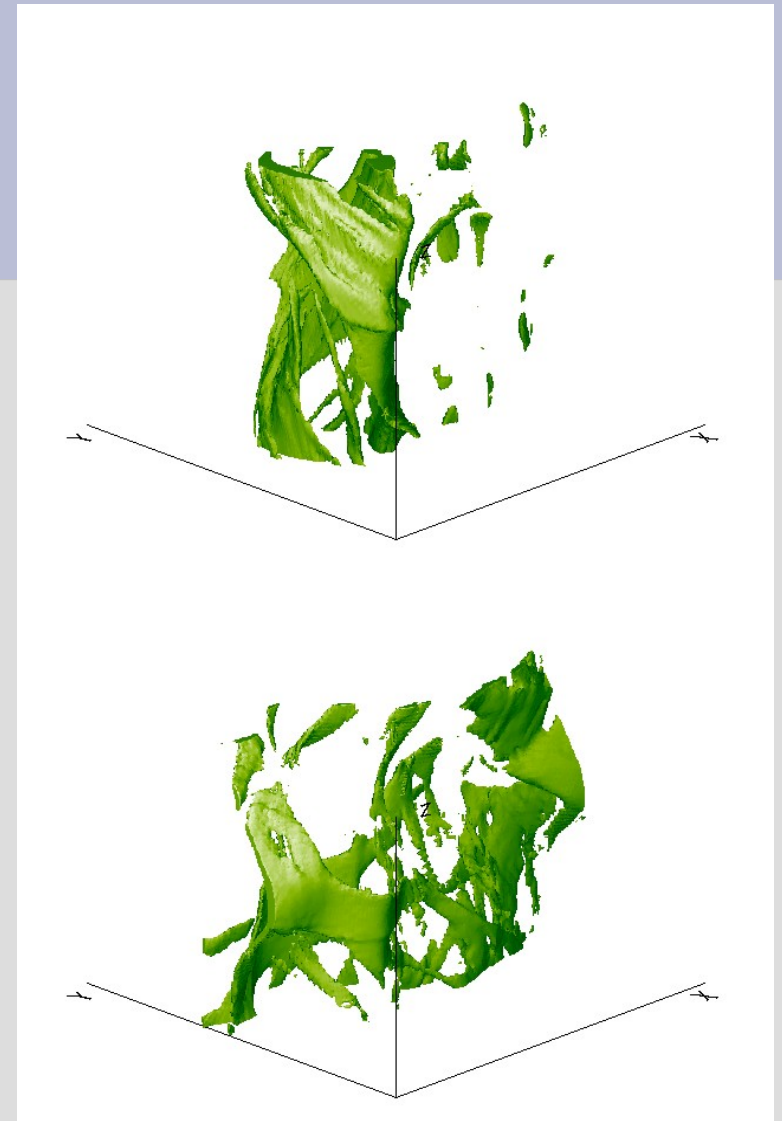
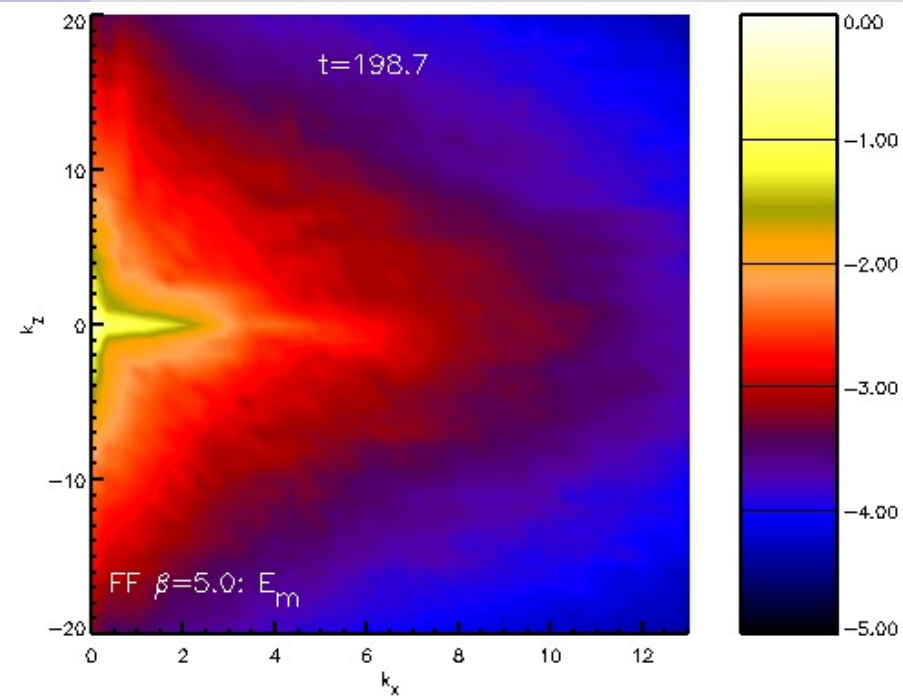


Plasma and current density structure during the non linear regime of the tearing instability

- Fundamental mode dominates the late stage of the system (coalescence signature)
- Anisotropic spectrum

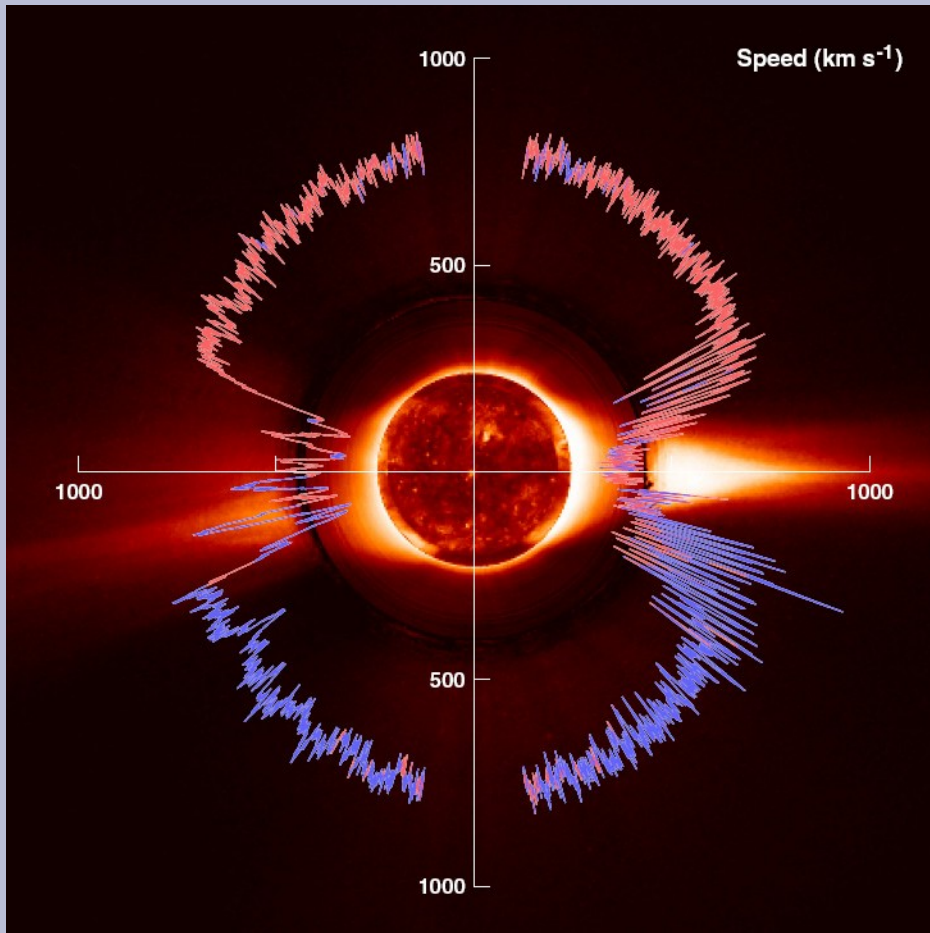
3-Force-Free configuration

- Coalescence is followed by a secondary instability.
- Differently from the previous case the system recover a more turbulent state



Magnetic energy spectrum is still anisotropic

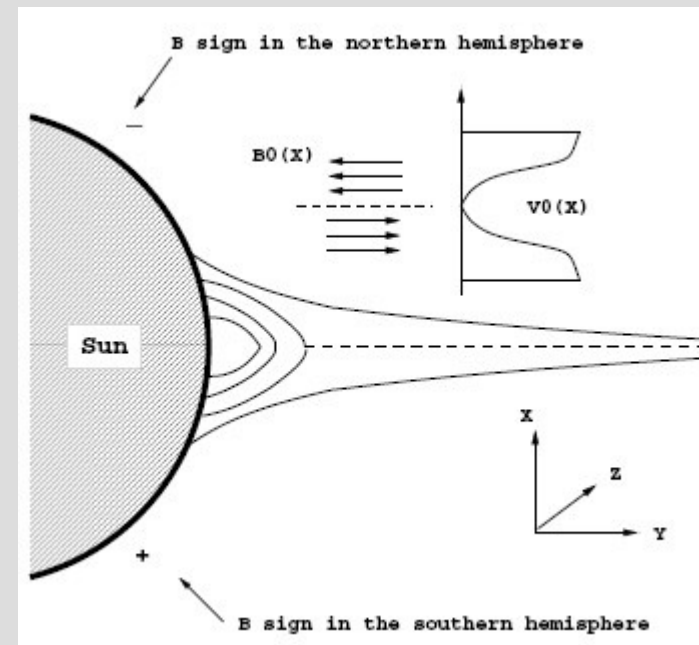
A Current Sheet embedded in a shear flow: A model of the Heliospheric Current Sheet in the solar wind



The solar wind: a supersonic flow originating from the Sun's atmosphere

Bimodal:
Fast at high latitudes, slower at low latitudes

Opposite magnetic polarities in the two hemispheres.



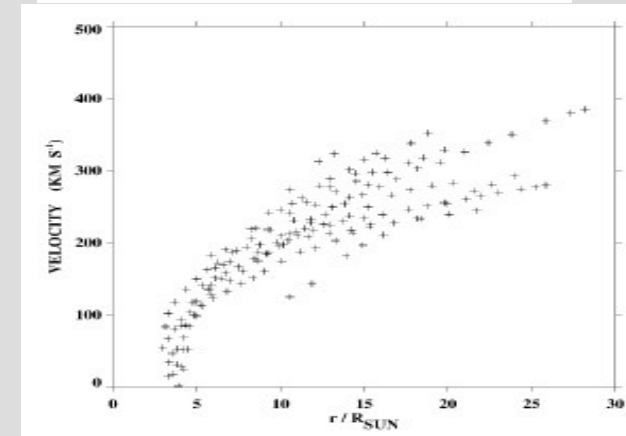
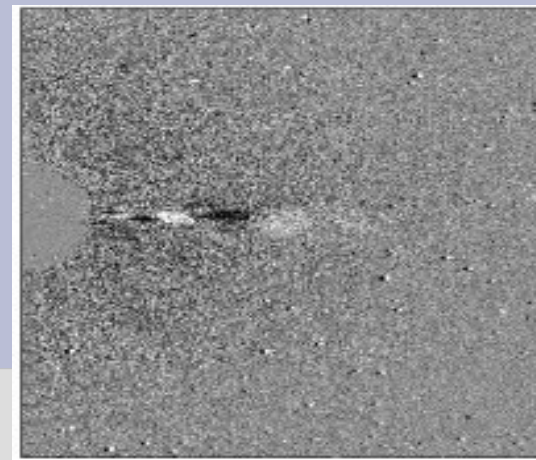
Ulysses measurements of the wind velocity and IMF polarity during its first journey from pole to pole. Superimposed are reproduced LASCO C2 coronagraph, EIT telescope onboard of SOHO and Mauna Loa coronagraph HAO.

A sketch of the large scale magnetic field and flow configuration in the inner heliosphere.

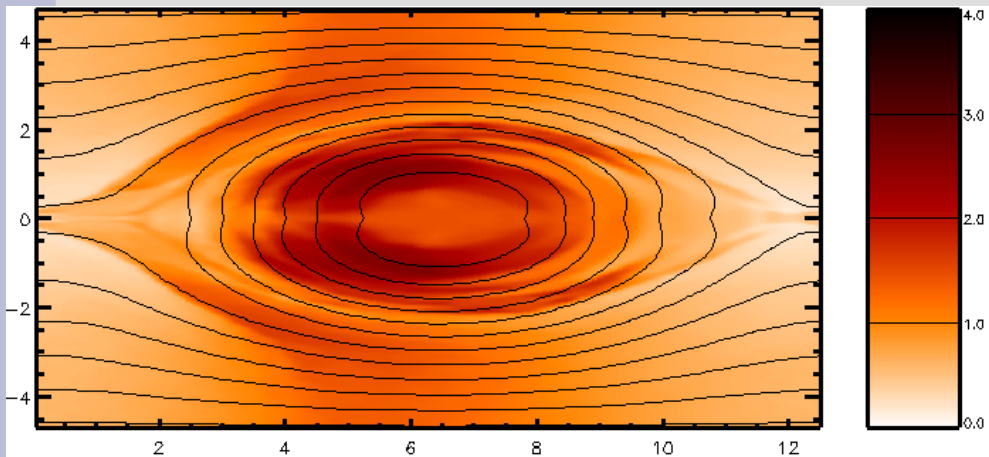
The Jet-Current Sheet model has been used to study the slow wind formation (Einaudi et al, 1999).

Plasmoids puffs observed in the helmet streamer (Einaudi et al., 1999, Einaudi et al., 2001)

Jet-Current sheet instability properties studied also taking into account Parker's spiral effects (Bettarini et al., 2006).



Plasmoid expulsion as seen from LASCO-C3 instrument on SOHO and scatter plot of plasmoid speed (Wang et al., 1998)



Formation of density enhancement during the later stage of the jet-current sheet configuration in a 2-D simulation performed with ECHO.

Model relevant also in other solar and astrophysical environments, e. g.: planetary tails (Sato and Walker, 1992), cometary tails (Cravens, 1997), galactic center non thermal filaments (Shore & Larosa, 1999), ...

3-D evolution of the Jet-Current sheet configuration

Different equilibria (pressure balance and force-free configurations) and different angles between the Interplanetary MF and the sheared flow

Plasma beta and Alfvén Mach number typical of the inner heliosphere.

$$M_a = 0.4$$

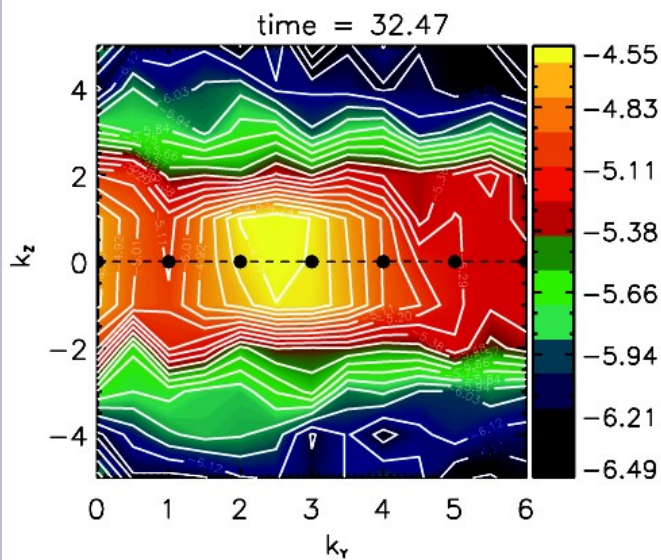
$$\beta = 0.02$$

$$M_s = 3.0$$

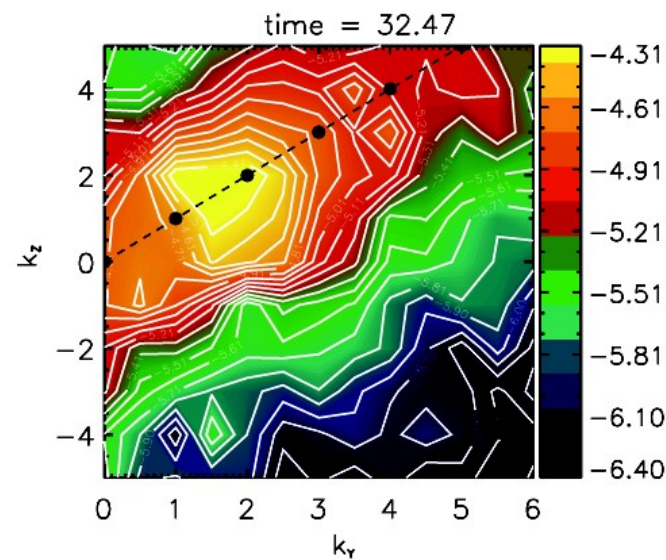
Linear phase

Characterized by the growth of modes parallel to the Interplanetary MF independently from the adopted equilibrium configuration.

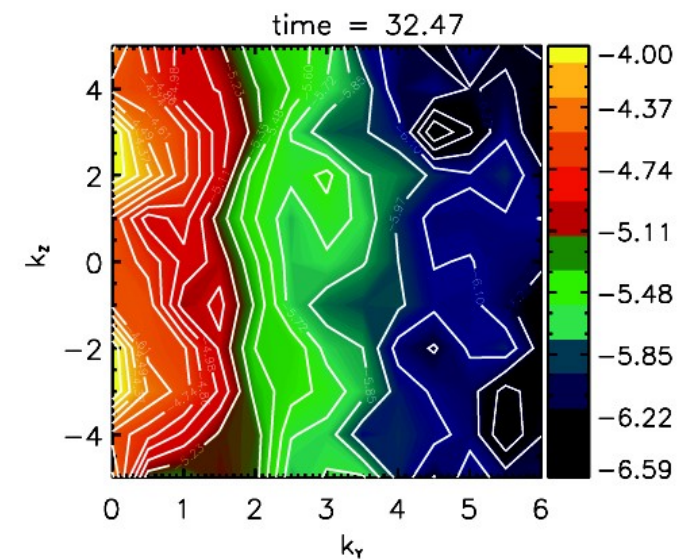
$$\sigma = 0$$



$$\sigma = \pi/4$$



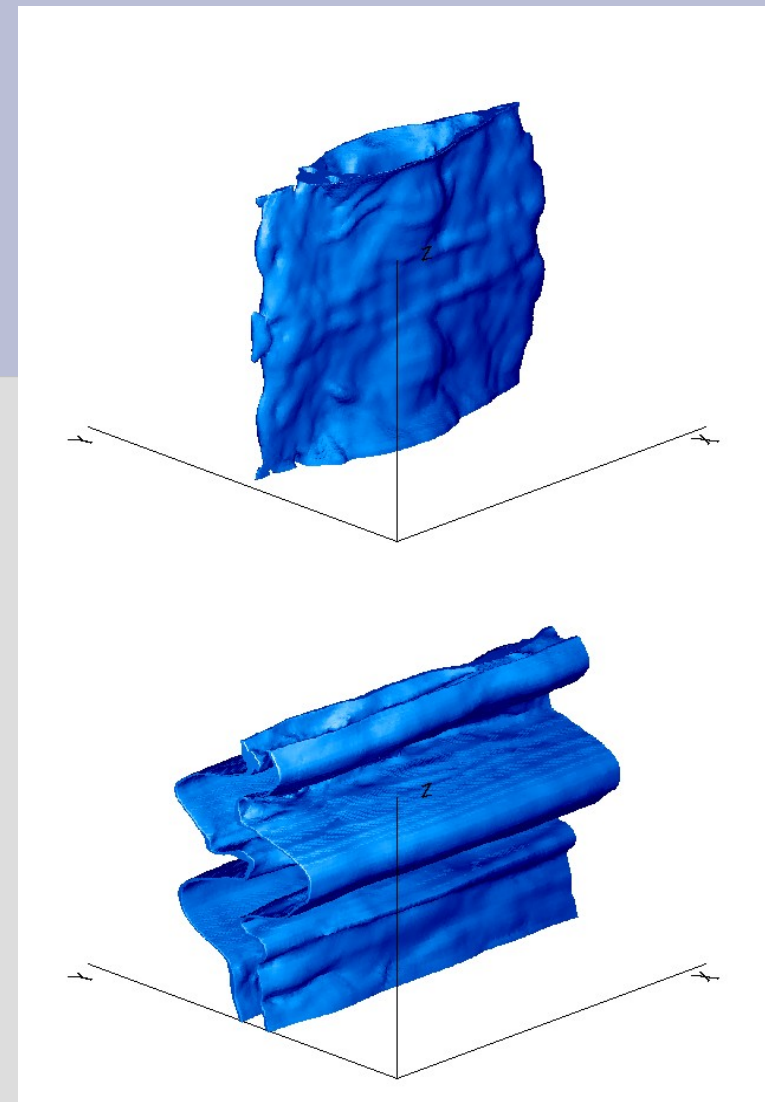
$$\sigma = \pi/2$$



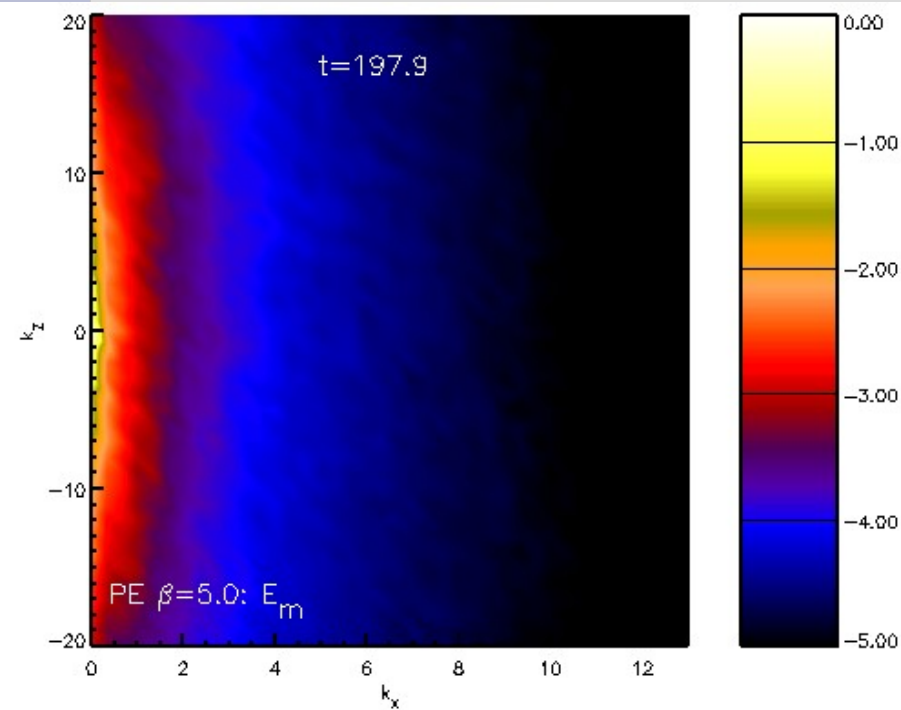
2-Pressure equilibrium configuration without guide field

Dynamic dominated by the secondary instability:

- Formation of magnetic islands by the tearing instability
- Secondary instability dominates the later stage of the current-sheet evolution. A final new 2D structure is recovered



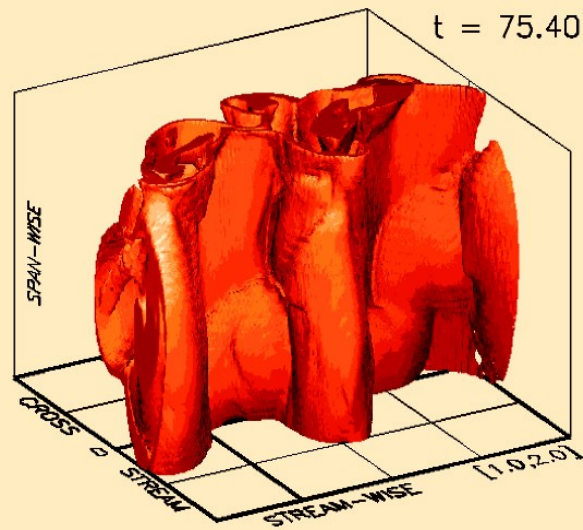
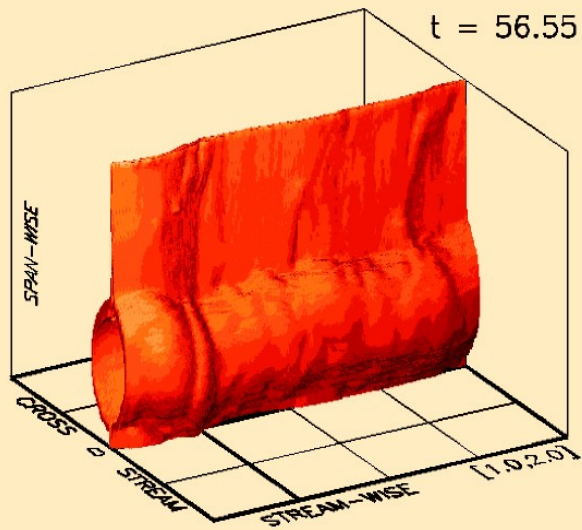
Plasma structure at 2 different times in the non linear phase of the tearing instability



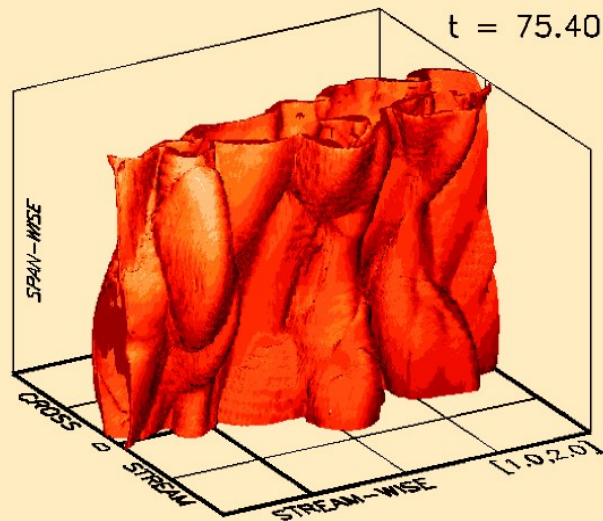
Magnetic energy spectrum is still anisotropic

Non linear phase: Transition to turbulence in the jet-current sheet configuration.

FF: $\sigma = \pi/2$

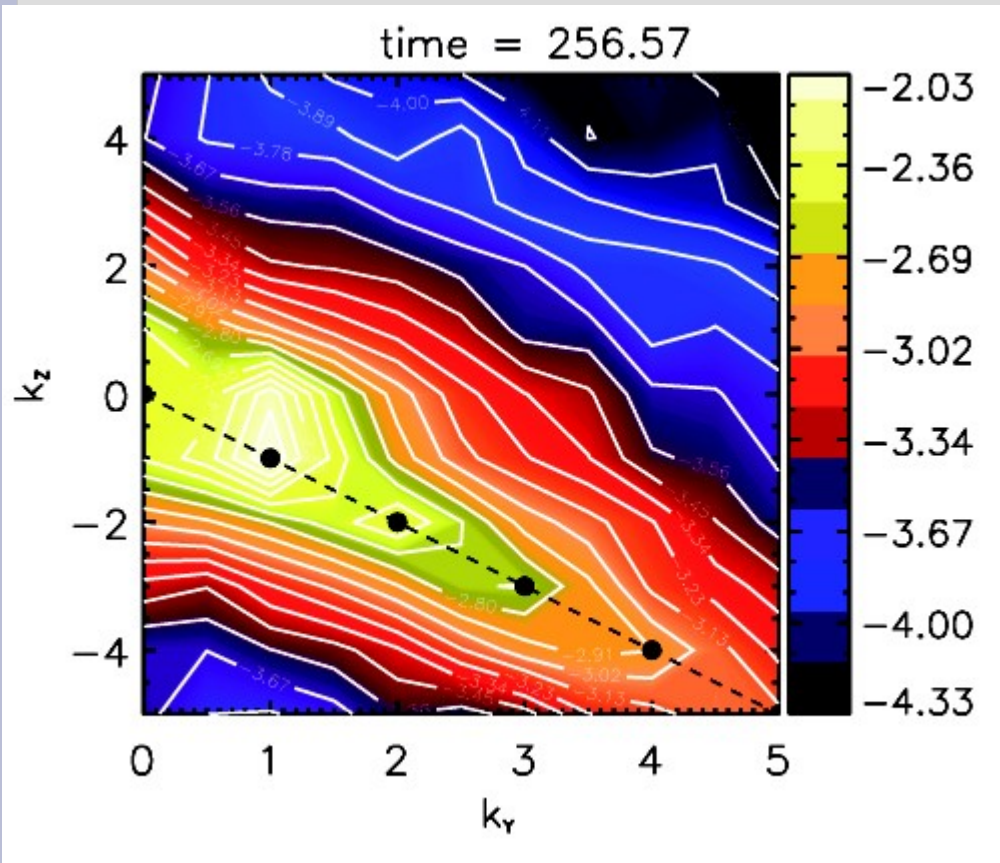


FF: $\sigma = 3\pi/8$

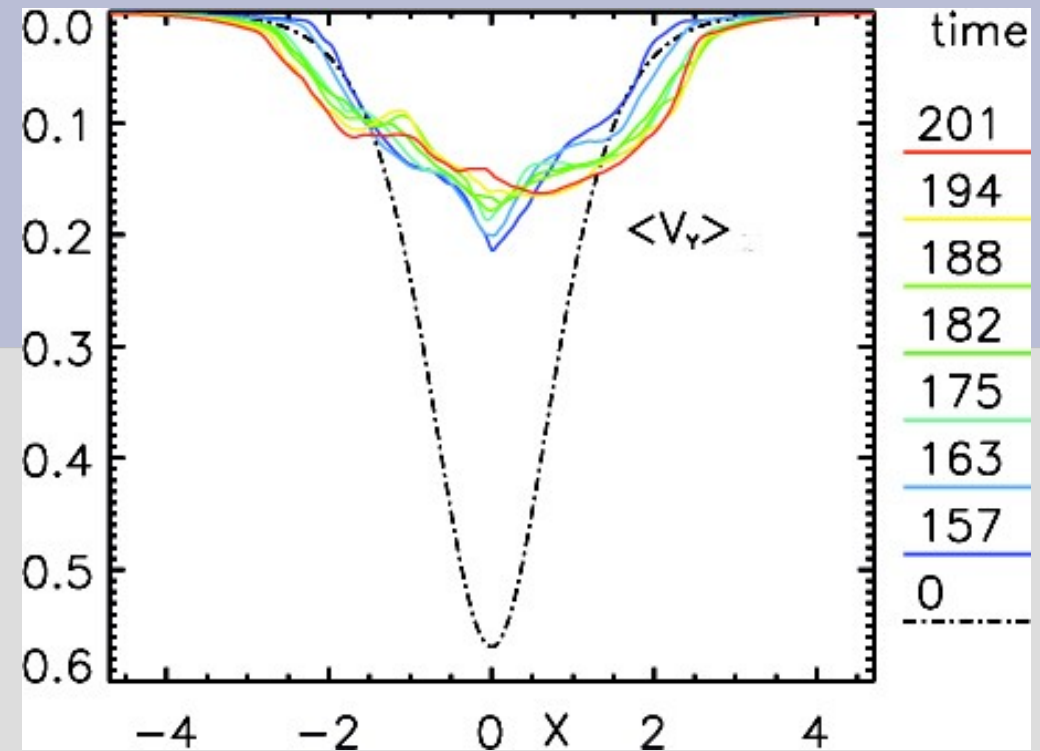


Also in this case transition to turbulence via the insurgence of a secondary instability (kinking of the magnetic island structure)

Acceleration of the wake during the non linear regime.



Magnetic energy spectrum for PE configuration $\sigma = \pi/4$



Wake velocity profile for PE configuration at different times. $\sigma = 3\pi/8$

Anisotropic magnetic spectra also in the non linear regime.

Conclusions

- We have designed an Eulerian Conservative High Order (ECHO) code where explicit diffusivity is taken into account and shock-capturing schemes are employed.
- The use of high-order schemes is a necessary ingredient in following the linear and non linear evolution of resistive and Kelvin-Helmholtz like instabilities.
- With ECHO we was able to follow the 3-D evolution of the tearing instability and those of a current-sheet embedded in a sheared flow, focusing on the onset of secondary instabilities and their transition toward a turbulent state.

References

- Bettarini, L., Landi, S., Rappazzo, F. A., Velli, M. and Opher, M., A&A 452, 321 (2006)
- Cravens, T. E., The physics of the solar system plasmas, Cambridge University Press (1997)
- Del Zanna, L., Bucciantini, N. and Londrillo, P., A&A 400, 397
- Del Zanna, L., Zanotti, O., Bucciantini, N. and Londrillo, P., A&A 473, 11 (2007)
- Einaudi, G., Boncinelli, P., Dahlburg, R. B. and Karpen, J. T., JGR 104, 521 (1999)
- Einaudi, G., Chibbaro, S., Dahlburg, R. B. and Velli, M., ApJ 547, 1167 (2001)
- Furth, H. P., Killen, J. and Rosenbluth, M. N., Phys. Fluids 26, 459 (1963)
- Dahlburg, R. B., Antiochos and S. K., Zang, T. A., Phys. Fluids B 4, 3902 (1992)
- Dahlburg, R. B. and Einaudi, G., Phys. Lett. A 294, 101 (2002)
- Landi, S., Londrillo, P., Velli, M. and Bettarini, L., Phys. Plasmas 15, 12302 (2008)
- Lele, S., K., JCP 103, 16 (1992)
- Liu, X.-D. and Osher, S., JCP 141, 1 (1998)
- Liu, X.-D., Osher, S. and Chan, T., JCP 115, 200 (1994)
- Londrillo, P. and Del Zanna, L., ApJ 530, 508 (2000)
- Onofri, M., Primavera, L., Malara, F. and Veltri, P., Phys. Plasmas 11, 4837 (2004)
- Sato, T. and Walker, R. J., JGR 87, 7453
- Shore, S. N. and Larosa, T. N., ApJ 521, 587 (1999)
- Suresh, A. & Huynh, H. T., JCP 136, 83 (1997)